The photocapacitance property of Cu/Cu_2O/Au sandwich structures

2002 Semicond. Sci. Technol. 17 1162

(http://iopscience.iop.org/0268-1242/17/11/305)

INSTITUTE OF PHYSICS PUBLISHING SEMICONDUCTOR SCIENCE AND TECHNOLOGY
Semicond. Sci. Technol. **17** (2002) 1162–1167 PII: S0268-1242(02)39258-7

The photocapacitance property of $Cu/Cu_2O/Au$ sandwich structures

Necmi Serin and Tülay Serin

Department of Engineering Physics, Engineering Faculty of Ankara University, 06100 Ankara, Turkey

E-mail: nserin@eros.campus1.ankara.edu.tr

Received 10 July 2002, in final form 30 August 2002
Published 4 October 2002
Online at stacks.iop.org/SST/17/1162

Abstract
We have carried out investigations into the photocapacitance property of domestically fabricated $Cu/Cu_2O/Au$ sandwich structures. For the fabrication, p-type cuprous oxide (Cu_2O) was grown on a copper sheet, and a transparent gold metal contact was applied on the cuprous oxide layer under a pressure of 1×10^{-6} Torr. The capacitance characteristics versus light intensity for different wavelengths in the visible region and the current–voltage characteristics of the sandwich structure were measured at a temperature of 15 °C. It was observed that the capacitance of the $Cu/Cu_2O/Au$ structure was significantly dependent on both wavelength and intensity of the light. The photocapacitance property of $Cu/Cu_2O/Au$ is discussed in terms of the effect of light on the interface states filled by charges and the change occurring in the imaginary part of the dielectric constant of the cuprous oxide created due to interface states.

1. Introduction

Cuprous oxide (Cu_2O), with a 2.0 eV forbidden energy bandgap and a cubic crystal structure, is among the former semiconductor materials used in the rectification of alternating current [1]. Since cuprous oxide is an ionic crystal, its type and electrical conductivity are strongly dependent on the oxygen pressure and on the method followed in its growing process [2]. Its resistivity varies in the range of 10^3–10^{13} Ω cm depending on the preparation condition. The crystal structure of cuprous oxide always creates difficulties in the understanding of its electronic conductivity mechanism. Thus, after 1947 silicon and germanium semiconductors became importance for semiconductor device fabrication. Recently, cuprous and cupric oxide have again become important since they are used in the composition of superconducting materials. The photoconductivity, photomemory and photovoltaic properties of cuprous oxide, which are investigated these days, have become attractive for some researchers [3–8].

Recently it has also been seen that the light-induced capacitance of a sandwich structure supplies important information about interface states and deep states. Thus, a new spectroscopy technique, called photocapacitance spectroscopy, has been developed as a popular method for investigations of deep states and surface states. Materials and sandwich structures which have the photocapacitance property are not common and there are only a small number of publications concerning these. The photocapacitance property has been observed in $CdZnS/CuInSe_2$, GaAs/AlGaAs and Bi-doped ZnO in some unique publications dealing with photocapacitance [9–11]. Although cuprous oxide also has similar photoelectric properties, we have found no studies on the photocapacitance of sandwich structures made of cuprous oxide. Thus, in this work we have aimed to research the photocapacitance property of the $Cu/Cu_2O/Au$ sandwich structure. In order to explain the physics of the photocapacitance on the electrical property of the $Cu/Cu_2O/Au$ sandwich structure, we have considered the concepts of the excitation of trapped electrons from filled interface states to the conduction band and the complex dielectric permittivity.

2. Experiment

A piece of copper sheet, having 99.99% purity, a thickness of 200 μm, and dimensions of 10×10 mm^2, was chemically cleaned by means of acetone (CH_3COCH_3), a mixture of deionized water and nitric acid (50% H_2O + 50% HNO_3). In order to obtain a very clean copper surface it was placed in a furnace at a temperature of 700 °C for 10 min

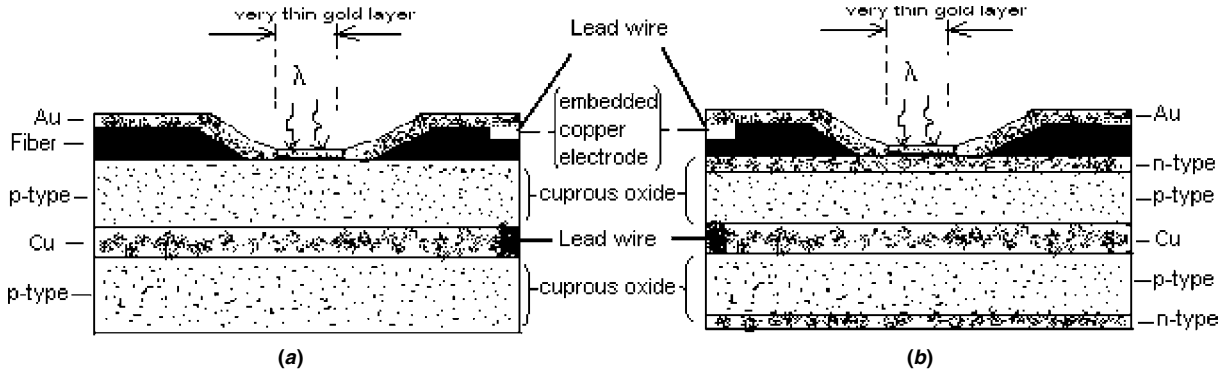

Figure 1. The structure of (*a*) $Cu/Cu_2O(\mathbf{u})/Au$ and (*b*) $Cu/Cu_2O(\mathbf{q})/Au$ devices.

[12, 13]. In this period the dried hydrogen gas was passed over the sample. As the sample was allowed to cool to room temperature, the very thin copper layer (consisting of oxides and chemical complexes such as dirts, with a thickness of 1–2 μm) was spontaneously cleaved from the surface with the help of hydrogen exposure, and thus a clean copper metal surface was obtained. In order to grow cuprous oxide, this copper metal was hung by a platinum wire in a furnace at a temperature of 1040 °C for 5 min. During this process and the following oxidation and annealing processes, the atmospheric pressure and relative humidity were 680 mmHg and 25%, respectively. At the end of this period, it was allowed to cool to room temperature. The samples were annealed in a furnace at a temperature of 600 °C for 5 min. Two different processes followed the annealing of the samples at 600 °C. Some of samples (referred to as unquenched Cu_2O) were allowed to cool in the room. In order to obtain a p/n junction within the Cu_2O layer, the other samples were quenched in deionized water [14]. In subsequent sections, the unquenched Cu_2O and quenched Cu_2O are referred to as $Cu_2O(\mathbf{u})$ and $Cu_2O(\mathbf{q})$, respectively. As a result, cuprous oxide (Cu_2O, thickness 32 μm) and cupric oxide (CuO, thickness 1 μm) were grown on both sides of the copper sheet and sandwiches of $CuO/Cu_2O(\mathbf{u})/Cu/Cu_2O(\mathbf{u})/CuO$ and $CuO/Cu_2O(\mathbf{q})/Cu/Cu_2O(\mathbf{q})/CuO$ were obtained. In order to remove the CuO thin layer on $Cu_2O(\mathbf{u})$ and $Cu_2O(\mathbf{q})$ both sandwiches were immersed in a mixture of hydrochloric acid (HCl) (20%) and sulfuric acid (H_2SO_4) (20%) for 1 min. After being rinsed with deionized water, they were immersed in concentrated nitric acid (HNO_3) for 10 s and then rinsed again with deionized water. In order to fix the samples, special fibre holders (as shown in figure 1) were fabricated.

A conical hole, for gold contact application, was formed in the fibre holder. The $Cu_2O(\mathbf{u})/Cu/Cu_2O(\mathbf{u})$ and $Cu_2O(\mathbf{q})/Cu/Cu_2O(\mathbf{q})$ sandwich structures were separately placed on these fibre holders by means of araldite. Only one side of the oxide layers $Cu_2O(\mathbf{u})$ and $Cu_2O(\mathbf{q})$ was used for the fabrication of the $Cu/Cu_2O(\mathbf{u})/Au$ and $Cu/Cu_2O(\mathbf{q})/Au$ structures. The other side of the oxide layers $Cu_2O(\mathbf{u})$ and $Cu_2O(\mathbf{q})$ was not used. As shown in figures 1(*a*) and (*b*), the lead wires were soldered to the copper parts in the $Cu_2O(\mathbf{u})/Cu/Cu_2O(\mathbf{u})$ and $Cu_2O(\mathbf{q})/Cu/Cu_2O(\mathbf{q})$ sandwich structures and to the copper electrode embedded in the fibre [13]. The transparent gold ohmic contacts were applied on the $Cu_2O(\mathbf{u})$ and $Cu_2O(\mathbf{q})$ layers under a vacuum of 1×10^{-6} Torr. As shown in figure 1, the sandwich structures of $Cu/Cu_2O(\mathbf{u})/Au$ and $Cu/Cu_2O(\mathbf{q})/Au$ were obtained.

In order to measure current–voltage and capacitance–light characteristics, the samples were placed in a closed box. All the measurements were carried out at zero bias, at a temperature of 15 °C and a frequency of 10 kHz. In order to be sure that the sample was not heated by illumination, its temperature was continuously checked by a thermocouple. A tungsten filament lamp and optical filters in 410, 434, 486, 589 and 656 nm wavelengths were used for the illumination of the sample.

3. Theory

At equilibrium, the bulk of a homogeneous semiconductor is neutral, and free of electric fields. Near a surface, however, conditions are different. Due to the interruption of the periodic lattice structure at the surface of a crystal [15], surface states exist within the forbidden gap. Uncompensated charges and fields are to be found there, in a thin space-charge layer under the surface. The thickness of this surface layer is usually of the same order as the value of the bulk Debye length, L_B, at room temperature [16]

$$L_B = [\varepsilon_r \varepsilon_0 kT/q^2(n_b + p_b)]^{1/2} \tag{1}$$

where ε_r, ε_0, k, T, q, n_b and p_b are the electrical permittivity of the semiconductor, the electrical permittivity of free space, the Boltzmann constant, the absolute temperature, the absolute value of the electronic charge, and the number of electrons and holes per unit volume in the bulk, respectively. The semiconductor surface exposed to the atmosphere is covered by a thin oxide, and there are usually charged centres, or surface states, at the interface between the semiconductor and oxide, and within the oxide itself. These charges lying in a surface layer give rise to electric fields. These produce a potential difference with respect to the bulk, which depends on position. These surface space-charge layers are classified as accumulation, flat band depletion layers and inversion layers [17]. Surface states are characterized by their density, N_t, per unit area and by their energy, E_i, at the flat band. The trapped charges at the interface states create a potential barrier for charge carriers and a majority charge-carrier depletion region around the interface. This potential barrier controls the conductance G of the sample which is given by the relationship

$$G = G_0 \exp(-qV_d/kT) \tag{2}$$

where qV_d is potential barrier created by interface states. This is found from the solution of the Poisson equation $\varepsilon(d^2\phi/dx^2) = -\rho(x)$. The result is expressed by means of the density of charge trapped at the interface as

$$qV_d = n_T^2/(8\varepsilon_r\varepsilon_0 N_d) \tag{3}$$

where n_T and N_d are the density of the charge trapped at the interface and the donor density, respectively. The capacitance of the depletion region per unit area by means of the number of the charge trapped at the interface is given [11]

$$C = (\varepsilon_r\varepsilon_0 N_d)/n_T. \tag{4}$$

The electrical permittivity ε_r of the semiconductor is defined by means of the relation $\mathbf{D} = \varepsilon_r\mathbf{E}$ where $\mathbf{D}$ and $\mathbf{E}$ are the displacement vector and the electrical field in the material, respectively. For nondispersive media, the value of ε_r is constant whereas in dispersive media it changes with the phase velocity of the light. For a homogeneous and isotropic material having electrical conductivity σ, the differential equation satisfied by the electrical field $\mathbf{E}$ is

$$-\nabla\cdot(\nabla\cdot\mathbf{E}) + \nabla^2\mathbf{E} = (\varepsilon_r/c^2)(\partial^2\mathbf{E}/\partial t^2) + (4\pi\sigma/c^2)(\partial\mathbf{E}/\partial t) \tag{5}$$

where c is the velocity of light. When the solution $\mathbf{E} = \mathbf{E}_0\exp(\mathbf{k}\cdot\mathbf{r} - \omega t)$ is substituted in equation (5) and after carrying out lengthy mathematical calculations, the electrical permittivity ε_r in the complex representation for metal

$$\varepsilon_r = [\varepsilon_{r1} + j(4\pi\sigma/c)] \tag{6}$$

is obtained, in the classic approximation, where the complex component is $\varepsilon_{r2} = 4\pi\sigma/c$. In the semiconductor case, $4\pi\sigma/c$ should be multiplied by a suitable constant.

In the quantum case, the derivation of the electrical permittivity ε_r in the complex representation is more complicated and long and it is simply given by the equation

$$\varepsilon_r = [\varepsilon_{r1} + (2\pi q/m\omega)^2 2N|P|^2 P(\hbar\omega)] \tag{7}$$

where ω is the angular frequency, ε_{r1} is the real part of the electrical permittivity, N is the number of centres, $P(\hbar\omega)$ is the distribution of energy differences $\hbar\omega = E_i - E_{0i}$, m is the mass of the free electron, and P is an element of the P_{0i} matrix (assumed to be constant) which provides a relation between the energy states E_{0i} and E_i [18–20].

4. Results and discussion

In order to determine the type of $Cu_2O(\mathbf{u})$ and $Cu_2O(\mathbf{q})$, the four-point probe method and the thermal galvanometric method were used [21, 22]. In the four-point probe method, four electrodes of a compact equipment were contacted on the surfaces of $Cu_2O(\mathbf{u})$ and $Cu_2O(\mathbf{q})$. Their type of resistivity was directly seen as p-type from the digital screen of the four-point probe equipment. In the thermal galvanometric method, the $Cu_2O(\mathbf{u})/Cu/Cu_2O(\mathbf{u})$ and $Cu_2O(\mathbf{q})/Cu/Cu_2O(\mathbf{q})$ layers were placed separately on the metal plates. The sharp electrodes contacted the surfaces of the $Cu_2O(\mathbf{u})$ and $Cu_2O(\mathbf{q})$ layers. Copper metal parts in the $Cu_2O(\mathbf{u})/Cu/Cu_2O(\mathbf{u})$ and $Cu_2O(\mathbf{q})/Cu/Cu_2O(\mathbf{q})$ sandwich structures were subsequently installed to a galvanometer by means of conductive wires. As the metal plate was heated, the directions of the thermoelectric current for the $Cu_2O(\mathbf{u})$ and $Cu_2O(\mathbf{q})$ layers were determined from the galvanometer. The same process was repeated for a crystal whose type was known. The directions of the thermoelectric current in the $Cu_2O(\mathbf{u})$ and $Cu_2O(\mathbf{q})$ layers were compared with the direction of the thermoelectric current in the known crystal. We concluded that both $Cu_2O(\mathbf{u})$ and $Cu_2O(\mathbf{q})$ were p-type. Since the thickness of the n-type region on the p-type region (discussed above) was very thin and it was spontaneously damaged during the application of sharp electrodes, the existence of the n-type region on the p-type region did not affect the p-type resistivity measurement. We can also see that these results are the same as those in the literature [23]. The current–voltage experiments have shown that the $Cu/Cu_2O(\mathbf{q})/Au$ sandwich structure behaved like a diode. When the rectification ratios of $Cu/Cu_2O(\mathbf{u})/Au$ and $Cu/Cu_2O(\mathbf{q})/Au$ at 1.5 V were compared with each other, it was observed that they were 2 and 12, respectively. These results indicated that a p/n junction with a significant diffusion barrier height was generated only within the quenched $Cu_2O(\mathbf{q})$ layer. In order to determine the origin and location of the n and p regions relative to the copper region in the $Cu/Cu_2O(\mathbf{q})$ structure, we used the polarity of the voltage applied to the $Cu/Cu_2O(\mathbf{q})/Au$ structure. In the current–voltage characteristic of the $Cu/Cu_2O(\mathbf{q})/Au$ structure, as shown in figure 2, it is seen that the current increased exponentially with increasing voltage at forward biases (copper positive and gold negative) and the increment of the current with increasing voltage was very small at reverse biases (copper negative and gold positive). These results indicate that the p-type section of the p/n junction in the $Cu/Cu_2O(\mathbf{q})/Au$ sandwich structure located on the copper and n-type section was near to the gold metal contact.

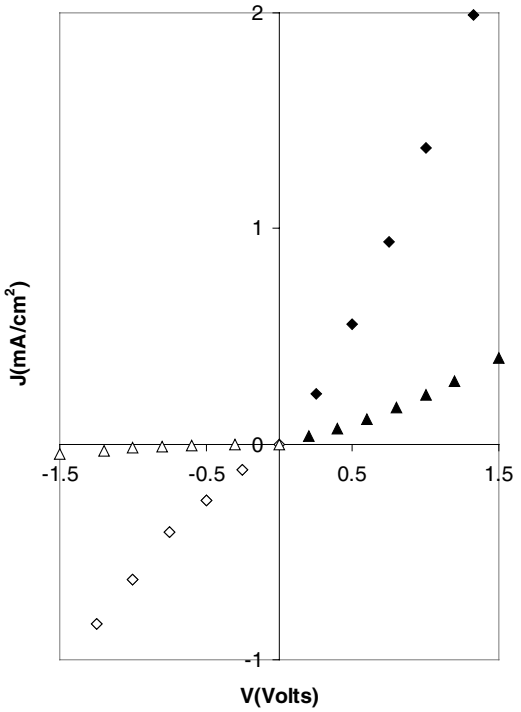

Figure 2. Current–voltage characteristics of the sandwich structure at reverse bias (◇, (−)$Cu/Cu_2O(\mathbf{u})/Au$(+); △, (−)$Cu/Cu_2O(\mathbf{q})/Au$(+)) and forward bias (◆, (+)$Cu/Cu_2O(\mathbf{u})/Au$(−); ▲, (+)$Cu/Cu_2O(\mathbf{q})/Au$(−)) at 15 °C.

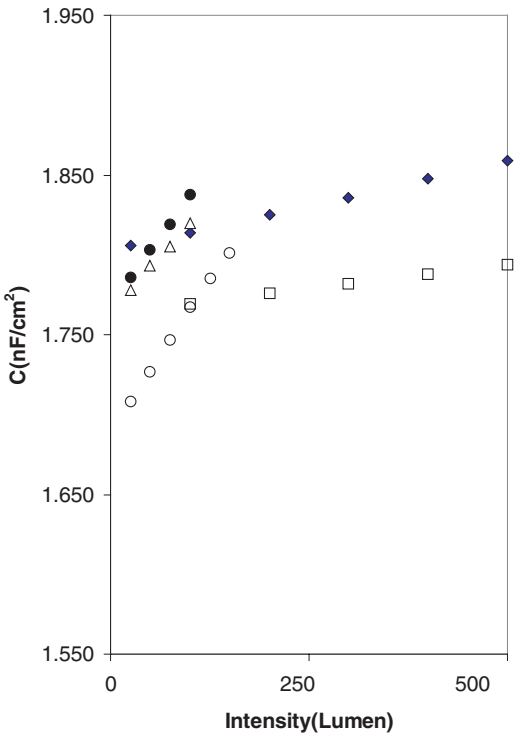

Figure 3. Capacitance of the $Cu/Cu_2O(\mathbf{q})/Au$ sandwich structure at zero bias versus light intensity for various wavelengths (nm) measured at 10 kHz: ♦, 410; ○, 434; △, 486; ●, 589; □, 656.

In the current–voltage characteristic of the $Cu/Cu_2O(\mathbf{u})/Au$ structure, as shown in figure 2, it is seen that the current nearly increased exponentially with increasing voltage at both forward and reverse biases and the differences in current values for forward and reverse biases were very small. Therefore, we consider that the p/n junction in $Cu/Cu_2O(\mathbf{u})$ is negligible. When the samples were illuminated by light through the thin metal gold contacts, we observed that the $Cu/Cu_2O(\mathbf{q})/Au$ structure had photocapacitance properties and the $Cu/Cu_2O(\mathbf{u})/Au$ structures did not.

The photocapacitance experiments were carried out on a large number of samples by means of an impedance bridge at 10 kHz. We observed that their reproducibilities were quite good, and that the capacitance of the $Cu/Cu_2O(\mathbf{q})/Au$ sandwich structure linearly increased with increasing light intensity (figure 3). It was seen that the increment in capacitance with light intensity was larger in 434, 486 and 589 nm wavelengths than in 410 and 656 nm wavelengths.

In the literature, the explanation of the photocapacitance mechanism of the metal/oxide/metal or metal/oxide/semiconductor/metal sandwich structures is made by means of interface states below the Fermi level in the metal/oxide or metal/semiconductor interfaces [11, 24, 25]. According to these papers, when the filled interface states are illuminated the trapped charge carriers are photoemitted into the conduction or valence bands depending upon the type of the material. For an n-type semiconductor, the states that are emptied by illumination have an energy from the bottom edge of the conduction band to a depth of the illuminating photon energy below the conduction band. Three electrical excitation processes during illumination are assumed to occur:

(i) Exciting electrons from the interface states to the conduction band decrease the amount of charge (n_T) trapped at the interface states. This decreases the barrier height and increases the capacitance.
(ii) Exciting electrons from bulk states to the conduction band increase the positive charge in the depletion region. This can be considered as an increase in the density of ionized donors, N_d. If the photoexcited electrons drift away from the interface, the barrier height decreases and the capacitance of the interface increases.
(iii) Band-to-band transitions increase the number of charge carriers in the valence and conduction bands and thus increase the conductivity of the sample. An additional electronic process that could occur is the excitation of electrons from the valence band into the empty interface or bulk states within the depletion region.

In order to interpret the photocapacitance effect in the $Cu/Cu_2O(\mathbf{q})/Au$ sandwich structure, the equivalent circuit, energy-band diagram and the representation for $Cu/Cu_2O(\mathbf{u})/Au$ and $Cu/Cu_2O(\mathbf{q})/Au$ sandwich structures are shown in figures 4(*a*) and (*b*) using the results obtained from the current–voltage characteristics. According to the equivalent circuit diagram shown in figure 4(*a*) for $Cu/Cu_2O(\mathbf{u})/Au$, the effective capacitance consists of only a geometric capacitance C_g ($=\varepsilon_r\varepsilon_0/d$) per unit area since the p/n junction is absent or negligible. The geometric capacitance per unit area of the $Cu/Cu_2O(\mathbf{u})/Au$ sandwich structure is theoretically calculated as 0.17 nF cm^{-2}. The effective capacitance, C_T, of the $Cu/Cu_2O(\mathbf{q})/Au$ sandwich structure shown in figure 4(*b*) consists of a parallel combination of the p/n junction capacitance of C_E, which is given by equation (4), and the geometric capacitance C_g. It is expressed by the equation $C_T = C_E + C_g$. When equation (4) is substituted for C_E and the expression of geometric capacitance is substituted for C_g, we obtain an expression for the effective per unit area capacitance of the $Cu/Cu_2O(\mathbf{q})/Au$ sandwich structure at zero bias

$$C_T = (\varepsilon_r\varepsilon_0 N_d)/n_T + \varepsilon_r\varepsilon_0/d. \qquad (8)$$

Equation (8) implies that the effective capacitance of the $Cu/Cu_2O(\mathbf{q})/Au$ sandwich structure should be greater, by the amount $(\varepsilon_r\varepsilon_0 N_d)/n_T$, than the geometric capacitance of the $Cu/Cu_2O(\mathbf{u})/Au$ sandwich structure. The measured value $C_T = 1.6$ nF cm^{-2} of the effective capacitance of the $Cu/Cu_2O(\mathbf{q})/Au$ sandwich structure confirms the contribution of the p/n junction capacitance to the effective capacitance of the $Cu/Cu_2O(\mathbf{q})/Au$ sandwich structure. It also explains the difference in capacitance range and behaviour of the $Cu/Cu_2O(\mathbf{u})/Au$ and $Cu/Cu_2O(\mathbf{q})/Au$ sandwich structures.

In view of the results obtained from the measurements, it can be said that the photocapacitance effect in the $Cu/Cu_2O(\mathbf{q})/Au$ sandwich structure is created by means of interface states below the Fermi level at the $Cu_2O(\mathbf{q})/Au$ interface. When the filled states at the $Cu_2O(\mathbf{q})/Au$ interface are illuminated by light through the thin gold contact (figure 1(*b*)), the trapped charge carriers at the interface states are photoemitted into the conduction band of the n-type Cu_2O region (as given in case (i)). The excited electrons, from the interface states at the $Cu_2O(\mathbf{q})/Au$ interface to the

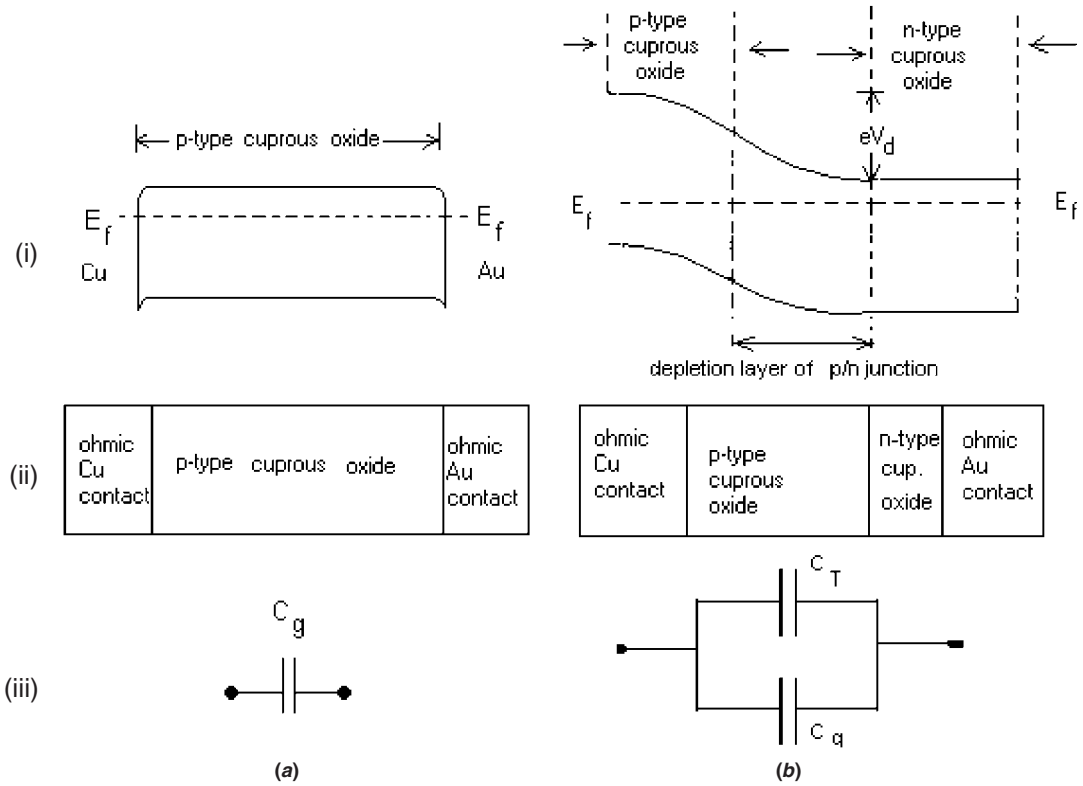

Figure 4. (i) Energy-band diagram, (ii) representation of the structure and (iii) the equivalent capacitance proposed for (*a*) Cu/Cu_2O(**u**)/Au and (*b*) Cu/Cu_2O(**q**)/Au sandwich structures.

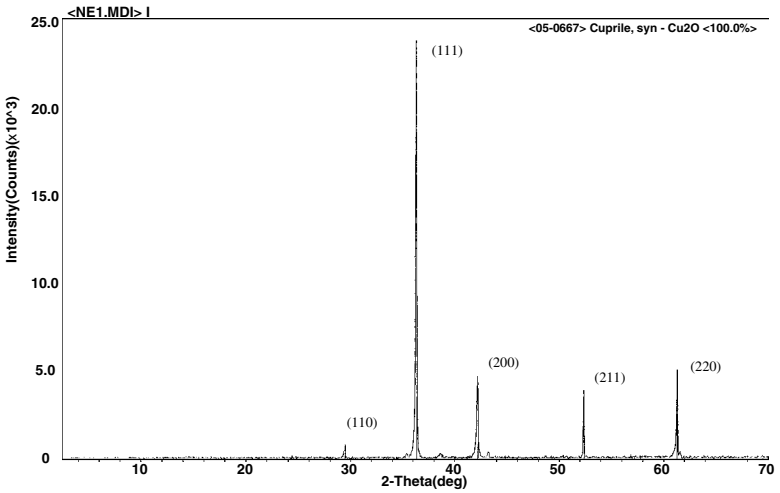

Figure 5. 2θ x-ray diffraction pattern of the cuprous oxide used in the fabrication of Cu/Cu_2O(**u**)/Au and Cu/Cu_2O(**q**)/Au.

conduction band decrease the amount of charge (n_T) trapped at the interface states. The decrement in the amount of charge trapped at the interface states causes an increment in the capacitance of the Cu/Cu_2O(**q**)/Au sandwich structure according to equations (3) and (4). On the other hand, since the number of electrons in the conduction band is increased, the electrical conductivity σ of the n-type Cu_2O region also increases. According to equations (6) and (7) the imaginary dielectric constant ε_{r2}, which results from the excitation of electrons from the interface states to the conduction band, also increases. The increment in the dielectric constant creates an additional increment in the capacitance of the Cu/Cu_2O(**q**)/Au sandwich structure according to equation (4). With these explanations, we can see that the change in the first term of equation (8), due to illumination, is dominant and that the source of the photocapacitance effect in the Cu/Cu_2O(**q**)/Au sandwich structure is the p/n junction formed by quenching in the Cu_2O(**q**) oxide. Since only the geometrical capacitance exists and the p/n junction is absent in the Cu/Cu_2O(**u**)/Au sandwich structure, the capacitance range of the Cu/Cu_2O(**u**)/Au sandwich structure is small. The changes caused in the electrical permittivity by light do not significantly affect the capacitance measurement.

The result of 2θ diffraction analysis is shown in figure 5. We observe that the characteristics have some peaks at the Miller index (110), (111), (200), (211) and (220), which

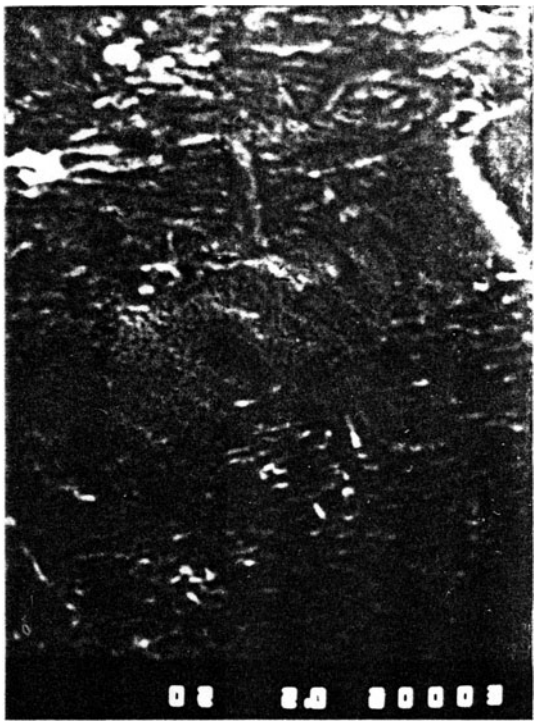

Figure 6. SEM image of the cuprous oxide surface.

correspond to the existence of cuprous oxide (Cu_2O) polycrystal. The analysis indicates that the cuprous oxide used in this study was polycrystalline and contained a random distribution of cuprous oxide single crystal. The amount of single crystals orientated in the ⟨111⟩ Miller index was effectively dominant. The scanning electron microscopy (SEM) image shown in figure 6 exhibits the dislocations and grains. Thus, we have decided that the capacitance characteristic under illumination, shown in figure 3, can be explained by means of the excitation of trapped electrons in the interface to the conduction band.

5. Conclusion

We have found that the photocapacitance of the $Cu/Cu_2O(\mathbf{q})/Au$ sandwich structure is significantly dependent on light intensity and wavelength. We conclude that, in the photocapacitance mechanism, the charges trapped in the interface states and in the p/n junction, created in the $Cu_2O(\mathbf{q})$ bulk by the quenching process, are dominantly effective. Thus, the photocapacitance property of the $Cu/Cu_2O(\mathbf{q})/Au$ sandwich structure has been explained by means of the amount of charge trapped in the interface states and the change occurring in the imaginary part of the dielectric constant of Cu_2O under illumination.

Acknowledgments

The authors would like to thank Phys. Eng. Öznur Çakir and Phys. Eng. Kadir Tuncel for the 2θ x-ray diffraction and SEM facilities, respectively.

References

[1] Othmer K 1963 *Encyclopedia Chem. Technol.* **4** 472
[2] Putley E H 1960 *The Hall Effect and Semiconductor Physics* (New York: Dover) p 214
[3] Bloem J 1958 *Philips Res. Rep.* **13** 167–72
[4] Gaplevkaya S P, Ezhik I I and Rvachev A L 1974 *Fiz. Tekn. Poluprov.* **8** 1605
[5] Olsen L C and Buhara R C 1978 *IEEE Transaction on Electron Devices* (New York: IEEE) p 1251
[6] Tomlinson W J and Yates J 1977 *J. Phys. Chem. Solids* **18** 1205
[7] Haydar A and Coret A 1978 *Phys. Status Solidi* a **48** 465
[8] Tapiero M, Noguet C, Zielinger J P, Schwab C and Pierrat D 1979 *Rev. Phys. Appl.* **14** 231
[9] Ahrenkiel R K 1986 *J. Appl. Phys.* **59** 181
[10] Rosencher R, Vodjdani N, Nagle J, Bois P, Costard E and Delaitre S 1989 *Appl. Phys. Lett.* **55** 1853
[11] Simpson J C and Cordaro J F 1991 *J. Appl. Phys.* **69** 4011
[12] Brower W S and Parker H S 1971 *J. Cryst. Growth* **8** 227
[13] Serin N, Serin T and Unal B 2000 *Semicond. Sci. Technol.* **15** 112–6
[14] Mizuguchi J 1976 *Japan. J. Appl. Phys.* **15** 907
[15] Sze S M 1969 *Physics of Semiconductor Devices* (New York: Wiley) p 444
[16] Schröder D K 1990 *Semiconductor Material and Device Characterization* (New York: Wiley) p 48
[17] Scott C G and Reed C E 1975 *Surface Physics of Phosphors and Semiconductors* (London: Academic) p 144
[18] Mancini N A and Quaercia I F 1977 *IV. Cource on Solar Energy Convension* (Trieste: International Atomic Energy Agency) p 160
[19] Abeles F 1972 *Optical Properties of Solids* (Amsterdam: North-Holland) p 292
[20] Haug H and Koch S W 1993 *Quantum Theory of the Optical and Electronic Properties of Semiconductors* (River Edge, NJ: Word Scientific) p 144
[21] Schröder D K 1990 *Semiconductor Material and Device Characterization* (New York: Wiley) p 2
[22] Seeger K 1991 *Semiconductor Physics* (New York: Springer) p 83
[23] Morgan D V and Howes M J 1974 *Phys. Status Solidi* a **21** 191
[24] Kamienieski E 1973 *Solid-State Electron.* **16** 1487
[25] Hasegawa E and Sawada T 1982 *J. Vac. Sci. Technol.* **21** 457